Published in final edited form as:

Psychophysiology. 2020 May ; 57(5): e13532. doi:10.1111/psyp.13532.

Effects of Eccentricity on the Attention-Related N2pc Component of the Event-Related Potential Waveform

Orestis Papaioannou, **Steven J. Luck**

University of California, Davis

Abstract

The N2pc ERP component has been widely used as a measure of lateralized visual attention. It is characterized by a negativity contralateral to the attended location or target, and it is thought to reflect contralaterally enhanced processing of attended information in intermediate-to-high levels of the ventral visual pathway. Given that receptive fields in these areas often extend a few degrees into the ipsilateral hemifield, we might expect that near-midline stimuli would be processed by both the contralateral and ipsilateral hemispheres, resulting in a diminished N2pc. However, little is known about the effect of eccentricity on the N2pc component. To address this gap in knowledge, we recorded the EEG while participants performed a discrimination task with stimuli presented at one of five eccentricities (0°, 0.05°, 1°, 2°, 4° and 8° between the inner edge of the stimulus and the midline). We found that N2pc amplitude remained relatively constant across eccentricities, including when the inner edge was at the midline, except that N2pc amplitude was reduced by more than 50% at the greatest eccentricity (8°). We also examined the contralateral positivity that often follows the N2pc. This positivity became progressively larger, and the transition from negative to positive occurred progressively later, as the eccentricity increased. These findings suggest that future experiments looking at the N2pc can use near-midline stimuli without compromising N2pc amplitude but should avoid large eccentricities. Implications about the neural generators of the N2pc are also discussed.

Keywords

EEG; ERP; N2pc; attention; eccentricity

1. Introduction

The N2pc is widely used event-related potential (ERP) index of covert visual-spatial attention. It is consists of a posterior contralateral negativity that begins approximately 200 ms after stimulus onset (Luck & Hillyard, 1994ab), and it is isolated by subtracting the activity in the electrodes ipsilateral to the target from the activity of their contralateral counterparts (e.g. subtracting the activity at the P7 electrode from the activity at the P8 electrode when the target is in the left visual field). This *contralateral-minus-ipsilateral*

Correspondence concerning this article should be addressed to Orestis Papaioannou, UC-Davis Center for Mind & Brain, 267 Cousteau Place, Davis, CA 95618. Contact: orpapa@ucdavis.edu.

Orestis Papaioannou, Center for Mind & Brain and Department of Psychology, University of California, Davis

Steven J Luck, Center for Mind & Brain and Department of Psychology, University of California, Davis

difference allows the experimenter to isolate the N2pc component from the many sources of brain activity that are not lateralized with respect to the location of the target.

Although the N2pc can be observed across a range of different physical stimuli, N2pc amplitude varies according to the vertical position of the target, with a substantially reduced N2pc for targets in the upper field compared to those in the lower field (Bacigalupo & Luck, 2019; Luck, Girelli, McDermott, & Ford, 1997). This may be a result of the anatomy of the neural generators of the N2pc, which are believed to lie in intermediate- to high-level areas of the ventral visual processing stream such as area V4 and the lateral occipital complex (Hopf et al., 2006, 2000). Due to the anatomical orientation of some of these areas (especially V4), stimuli in the lower visual field are likely to activate dorsolateral sites close to the scalp, leading to a prominent ERP signature. Stimuli in the upper visual field, on the other hand, would be expected to activate sites located on the ventral surface of the occipital lobe, leading to an attenuated signal at the scalp (Luck, 2012).

The distribution of receptive fields (RFs) in these ventral areas makes it possible that N2pc amplitude would also vary as a function of the distance of the target from the midline. This is because RFs in these areas are heavily weighted towards the fovea (Dumoulin & Wandell, 2008; also see Gross, Rocha-miranda, & Bender, 1972 for RFs in anatomically equvalent areas in macaques). The foveal concentration of RFs in these areas means that objects in the periphery are represented by relatively few neurons and would be expected to produce less overall activity than stimuli near the midline (see figure 1). We would therefore expect that the N2pc would be smaller for targets presented far from the fovea.

On the other hand, many RFs in these areas extend into the ipsilateral hemifield, so it is possible that stimuli presented close to the midline would produce similar activity in the contralateral and ipsilateral hemispheres. This would decrease the apparent amplitude of the contralateral-minus-ipsilateral difference wave that is used to isolate the N2pc component (see figure 1). However, Chelazzi, Duncan, Miller, & Desimone (1998) found that neurons in inferior temporal cortex that responded vigorously to individual stimuli whether they were in the contralateral or ipsilateral hemifield acted very differently when contralateral and ipsilateral stimuli were presented simultaneously. For simultaneous stimuli, the neurons responded almost exclusively on the basis of the features of the contralateral object. If this contralateral bias for simultaneous stimuli is generally true for the sources of the N2pc, then it would allow for a large N2pc amplitude even when the target is near the midline, as long as there is a distractor present across the midline.

Knowing the effects of eccentricity on N2pc amplitude would have important practical implications for the design of future N2pc experiments, because it would allow researchers to maximize the amplitude of the N2pc and thereby achieve greater sensitivity and statistical power. Moreover, if N2pc amplitude is indeed affected by eccentricity, then care should be taken when comparing conditions in which the stimuli differ in eccentricity. Lastly, if a robust N2pc can be obtained for near-midline stimuli, then this makes it possible to use the N2pc in studies examining complex stimuli that might be difficult to discriminate when presented far from the midline (e.g., faces) due to the loss of visual acuity in parafoveal and peripheral areas.

Schaffer, Schudo & Meineke (2011) provided some evidence concerning the effect of eccentricity on the N2pc component. They manipulated the eccentricity (from 2°−7°) of a single patch which differed in texture from the background, and they reported that N2pc amplitude decreased slightly with increasing eccentricity. However, the target patch was physically different from the background, making it difficult to know whether the observed effect reflected attention-related N2pc activity or lateralized low-level sensory activity that was present during the N2pc time window.

As illustrated in Figure 2, the present study investigated the effects of eccentricity with a more typical N2pc paradigm, in which stimuli of different colors were presented on opposite sides of the display. Attention was directed to one of the two colors for a given trial block by means of an instruction at the beginning of the block (following the *Hillyard Principle*; see Luck, 2014). We systematically varied the eccentricity of the target and distractor objects, which ranged between 0° and 8° from the midline to the object's inner edge.

Manipulations of eccentricity are complicated by the fact that visual acuity and cortical area are both reduced as the eccentricity increases. Consequently, if the stimuli are the same physical size at the different eccentricities, they will be processed by fewer neurons and with lower acuity at the greater eccentricities. We addressed this by including a set of trials in which the stimulus size was increased for greater eccentricities according to the cortical magnification factor, thus approximately equating cortical area across eccentricities[1]. However, one might argue that this confounds eccentricity with the physical size of the stimuli, so we also included a set of trials where the stimuli were the same physical size for all eccentricities. Together, these two sets of trials allowed us to test whether any effects of eccentricity on N2pc amplitude might be a result of changes in stimulus size or cortical area.

We also investigated the effect of eccentricity on a less commonly reported but related component, which we term the *post-N2pc positivity* (PNP)[2]. This is a contralateral positivity that follows the N2pc (starting approximately 300 ms after stimulus onset) in some experiments. It has been suggested that the PNP might reflect attentional disengagement from the target stimulus (Sawaki, Geng & Luck, 2012), but more experiments are needed to narrow down the functional significance of the component. Any differences in the effects of eccentricity on the N2pc and the PNP may be useful in identifying the underlying neural generators and in dissociating the effects of other manipulations on these two components.

[1]The cortical magnification factor used in the present study was derived from area V1 and may not exactly capture the cortical magnification found in higher-order areas of visual cortex. Thus, this was only an approximate method for equating cortical eccentricity within the areas that likely generate the N2pc component.

[2]The name of the positivity that follows N2pc varies across studies. Sawaki et al. 2012 referred to it as P_D (distractor positivity), assuming that it was identical to an earlier component that has been shown to reflect the suppression of distractors (Hickey, Lollo, & Mcdonald, 2008). Hilimire & Corballis (2014) referred to a post-N2pc positivity as *Ptc* (posterior-temporal positivity), citing a more temporal distribution than the N2pc. Because a true distractor positivity would be found ipsilateral to the target and is inconsistent with the effect observed in the present experiment, and we did not observe a voltage focus in the temporal lobe, we will use the purely descriptive term *post-N2pc positivity* (*PNP*) to refer to any posterior positivity that immediately follows the N2pc.

2. Method

2.1 Participants

The final sample consisted of 20 participants (14 female), which is currently the default a priori sample size for within-group ERP experiments in our laboratory. Four additional participants were tested but were excluded as described in section 2.1.2. The participants were between the ages of 18 and 30 (mean = 20.7, SD = 2.3), with normal or corrected-to-normal visual acuity and no known neurological issues. Consent was obtained at the start of the experiment, and participants received monetary compensation. The protocol was approved by the University of California, Davis Institutional Review Board.

2.1.2 Exclusion Criteria—Participants were excluded if they met any of three a priori exclusion criteria: i) if they did not complete the recording session, either due to technical difficulties (1 participant) or because they opted to terminate the experiment early (1 participant); ii) if more than 25% of trials were rejected because of artifacts (0 participants); iii) if there was excessive alpha (more than 5μV peak to peak for more than 1 cycle) during the pre-stimulus baseline of the averaged ERPs (2 participants).

2.2 Stimuli and Procedure

Stimuli were presented on a Dell 2408WFP monitor (refresh rate = 60 Hz) using PsychToolbox (Brainard, 1997; Pelli, 1997). The participants viewed the monitor from a distance of 100 cm in a dimly lit room. The monitor had a grey background (0.31 cd/m^2, x = 0.31, y = 0.42) and contained a white fixation cross (11.7 cd/m^2, x = 0.30, y = 0.33) that was visible at all times. The monitor delay (30 ms) was measured with a photodiode, and the event codes were shifted to align with the actual stimulus onset time.

As illustrated in Figure 2, each display consisted of a red shape presented on one side of the screen and a blue shape presented on the other, with the side chosen randomly on each trial. Each shape was randomly and independently chosen on each trial to consist of a hemicircle or a rectangle (the left or right half of a square). Each shape was flanked above and below by a purple square or circle. All colors were approximately isoluminant. The standard PsychToolbox anti-aliasing algorithm was used to reduce stimulus artifacts that become apparent with foveal stimuli.

Stimulus eccentricity was varied experimentally, with the inner edge of each shape set to be 0° (i.e., with the two shapes touching on the midline), 0.048°, 0.952°, 1.905°, 3.810°, or 7.619° from the midline. For convenience, these are henceforth rounded to 0°, 0.05°, 1°, 2°, 4°, and 8°, respectively. The two stimuli in a given display were presented with equal eccentricities.

On non-magnified trials, the red and blue shapes were 1.71° in height and 0.86° in width, whereas the purple shapes were 0.79° in both dimensions. On magnified trials, all shapes were scaled by the cortical magnification factor (Rovamo & Virsu, 1979) (1×, 1.0145×, 1.29×, 1.5801×, 2.1608×, and 3.3261× for the 0°, 0.05°, 1°, 2°, 4°, and 8° eccentricities, respectively).

The task was split into four blocks. In each block, participants were instructed to attend to either the red shapes or the blue shapes. We alternated between attend-red and attend-blue in an ABAB design, with the starting color counterbalanced across participants.

Each stimulus display was presented for 800 ms, followed by a 700±100 ms blank period (rectangular distribution) during which only the fixation point was visible. Participants were instructed to press one of two buttons on a gamepad on each trial to indicate whether the shape of the attended color was a half circle or a half square, responding as fast as they could while remaining accurate. They were told to look at the fixation point at all times, and the experimenter provided additional feedback if eye movements were frequently observed. Each block consisted of 768 trials, with eccentricity (0°, 0.05°, 1°, 2°, 4°, and 8°) and magnification (magnified and non-magnified) randomized across trials. Across the four blocks, there were 256 trials for each combination of eccentricity and magnification.

2.3 EEG Recording and Analysis

EEG signals were recorded using a Brain Products actiCHamp system, with electrodes at 27 scalp locations (FP1, FP2, F3, F4, F7, F8, C3, C4, P3, P4, P5, P6, P7, P8, P9, P10, PO3, PO4, PO7, PO8, O1, O2, Fz, Cz, Pz, POz, Oz) as well as the left and right mastoids. The electrooculogram (EOG) was recorded simultaneously from an electrode placed 1 cm lateral to the outer canthus of each eye and from an electrode below the right eye. The data were recorded in single-ended mode and digitized at 500 Hz after application of an online cascaded integrator-comb anti-aliasing filter with a half-power cutoff at 260 Hz. Impedances were kept under 50 kΩ.

Offline analysis was performed using the EEGLAB (Delorme & Makeig, 2004) and ERPLAB (Lopez-Calderon & Luck, 2014) open source Matlab packages. The recorded signals were down-sampled to 250 Hz, and a noncausal Butterworth high-pass filter was applied (half-amplitude cutoff = 0.01 Hz, slope = 12 dB/octave). The scalp EEG signals were referenced to the average of the left and right mastoids, and the EOG signals were referenced into bipolar horizontal EOG (right minus left outer canthus) and vertical EOG (below the right eye minus Fp2) derivations. Before artifact correction and segmentation, periods of EEG data that corresponded to breaks or contained very large voltage deflections were removed to improve the artifact correction process that occurred next.

Artifact correction was performed using independent component analysis (ICA), and components corresponding to horizontal and vertical eye movements were identified on the basis of the correspondence of their shape, timing, and topography to the single-trial EOG signals. These components were then removed (typically 2–3 components per participant).

Artifact correction was supplemented with artifact rejection. We eliminated trials that contained large artifactual deflections (>250 μV) in any channel following artifact correction. We also removed trials on which the participants blinked or moved their eyes at a time that might impact the sensory input using a modified version of the technique described in Woodman & Luck, 2003. Specifically, we applied a step-function algorithm (Luck, 2014) to the uncorrected vertical and horizontal bipolar EOG channels to identify trials containing eye blinks and eye movements during the baseline period and the N2pc measurement

window, and we then excluded those trials from the averaged ERPs. The algorithm was applied at a time window spanning from −200 to 300 ms relative to stimulus onset, but was most sensitive to eye movements occurring between −150 to 250 ms. No more than 25% of total trials were rejected during the artifact rejection procedures for any participant.

The average residual HEOG activity (without artifact correction) is shown in figure 3. The average deflection was less than 3.2 μV for all participants and all timepoints before or during our N2pc time window, which would correspond to an average eye movement of less than ±0.1° (on the basis of the normative values provided by Lins, Picton, Berg, & Scherg, 1993). Even without ICA correction, these eye movements would produce a voltage deflection of less than 0.1 μV at any of the electrodes used in our analyses (on the basis of the propagation factors provided by Lins et al.).

Eye movement artifacts occurring after ~250 ms were not rejected from the analysis because this would have led to a large number of rejected trials, resulting in the exclusion of a large number of participants because of our a priori procedure of eliminating anyone for whom more than 25% of trials are rejected (Luck, 2014). However, previous research has shown that ICA is quite effective at minimizing the direct effects of eye movements on the EEG (Drisdelle, Aubin, & Jolicoeur, 2017; Mennes, Wouters, Vanrumste, Lagae, & Stiers, 2010). Eye movements may also cause indirect effects because they change the lateralization of the sensory input. However, the data in Figure 3 show that the average deviation in eye position during the PNP period was a small fraction of the eccentricity of the stimuli (e.g., ±0.5° when the stimuli were presented at an eccentricity of 8°). This is discussed further in sections 3.2.2 and 4.

Averaged ERPs were computed with an epoch of −200 to 600 ms relative to stimulus onset and baselined to the pre-stimulus portion of the epoch. To isolate the N2pc, we calculated a contralateral-minus-ipsilateral difference wave by subtracting the response of the electrodes in the hemisphere ipsilateral to the target from that of the electrodes in the contralateral hemisphere and then averaging across the left and right hemispheres. To simplify the analysis and reduce the potential for Type I errors, the difference waves were averaged across channels into an a priori cluster of interest (COI) consisting of all posterior and occipital electrodes (P3/P4, P5/P6, P7/P8, P9/P10, PO3/PO4, PO7/P08, and P1/02).

To identify appropriate measurement windows that reflect the timing of the observed components without artificially inflating the size of our effects, we used a variant of the “collapsed localizer” technique described by Luck & Gaspelin (2017). Specifically, we collapsed the contralateral-minus-ipsilateral difference waves across eccentricities and across the magnified and non-magnified trials, and we then performed a mass univariate analysis (Groppe, Urbach, & Kutas, 2011a, 2011b) to find the cluster of time points during which a given component was significantly different from zero. We used the cluster mass approach, which entailed testing each time-point against zero with a one-sample t test, and then identifying temporal clusters of two or more adjacent time-points that were individually significant. The t values in each cluster were summed together to determine the mass of the cluster. This cluster mass was compared to a null distribution of cluster masses, created by permuting the data in a way that was equivalent to randomizing the labels indicating the side

of the target stimulus (see Groppe, Urbach, & Kutas, 2011a, 2011b for more details about the technique and the rationale behind it). If the non-permuted cluster mass was within the top 5% of the null distribution created by the random permutations, then the cluster as a whole was deemed significant. By collapsing across our conditions prior to performing this analysis, we were able to identify the time windows in which the N2pc and PNP components were present in an unbiased manner.

We decided a priori to test only time points within 100–550 ms of stimulus onset, because any clusters at earlier or later time points are unlikely to reflect our components of interest. We found two significant clusters that fell within that range, spanning 140–252 ms and 300–444 ms post stimulus onset correspondingly, which are consistent with the timing of the N2pc and PNP components as reported in the literature. The boundaries of these clusters were then used to define the time windows used to measure the N2pc and PNP components for each individual combination of eccentricity and magnification. These amplitudes were quantified as the mean voltage within the time period, averaged across the electrodes in the cluster of interest.

2.4 Time-Frequency Analysis

The N2pc is sometimes accompanied by a lateralized suppression of alpha-frequency EEG activity (Bacigalupo & Luck, 2019; Worden, Foxe, Wang, & Simpson, 2000), and we analyzed this activity using time-frequency analysis to see if it varied across eccentricities. Because this was a secondary analysis, the methods and results are provided in online supplementary materials.

2.5 Statistical Measurements and Analyses

The amplitude of the N2pc and PNP components was defined as the mean amplitude of the contralateral-minus-ipsilateral waveform at our cluster of interest across the first time-window (140–252 ms) or the second time window (300–444 ms), respectively. Measurements of latency were used only in post-hoc analyses, the details of which can be found in section 3.3.

Behavioral measures included response accuracy, measured as the proportion of responses that were correct, and reaction time, measured for correct responses. Trials where the participant responded incorrectly or did not respond in time were coded as incorrect for the purpose of accuracy measures and were ignored for the purpose of reaction time measures.

Statistical analysis was conducted using the R software package (R Core Team, 2016). All ANOVAs were conducted using the ez package for R (Lawrence, 2013). Family-wise false discovery rate (FDR) corrections were performed for follow-up t-tests (Benjamini, Krieger, & Yekutieli, 2006), and the Huynd-Feldt correction for nonsphericity was used for ANOVA factors with more than 2 levels. Where the latter was used, we report the uncorrected F-ratio and degrees of freedom, but the post-correction p-value (denoted as p_{HF})

Initial analyses revealed no interaction between magnification and eccentricity for either time window (N2pc: $F(5) = 0.55$, $p_{HF} = .733$; PNP: $F(5) = 0.53$, $p_{HF} = .732$). Therefore, for

the sake of simplicity, we collapsed across magnification levels for the main analyses. Supplementary Figure S1 shows the non-collapsed data.

3. Results

3.1 Behavioral Results

Figure 4 summarizes the behavioral results. Shape discrimination accuracy was near ceiling in all conditions and will not be described further.

Mean reaction time (RT) followed a non-monotonic pattern, with longer RTs at the smallest and largest eccentricities, especially for the non-magnified stimuli. This pattern was verified using a two-way repeated measures ANOVA with factors of eccentricity and magnification. The overall change in RT across eccentricities led to a significant main effect of eccentricity ($F(5,95) = 16.7$, $p_{HF} < .001$), and the overall slower RTs for the magnified stimuli led to a significant main effect of magnification ($F(1,19)=55.7$, $p < .001$). The greater effect of magnification at the large eccentricities led to a significant interaction between eccentricity and magnification ($F(5,95) = 12.2$, $p_{HF} < .001$).

It is not clear why RTs were slower for the magnified stimuli than for the non-magnified stimuli, which is the opposite of what might be expected given that the magnified stimuli were larger than the non-magnified stimuli, especially at the larger eccentricities. One possibility is that the variation in physical size across eccentricities for the magnified stimuli slowed the response selection process, as might be expected on the basis of Logan's instance theory of automaticity (Logan, 1998). Another possibility is that the slower RTs were a consequence of slower processing of larger stimuli in the periphery (Carrasco, Mcelree, Denisova, & Giordano, 2003).

3.2 ERP Amplitude Results

Grand average contralateral-minus-ipsilateral difference waves waveforms are shown in Figure 5. We begin with an overview of the waveforms and then provide the statistical analyses. The parent waveforms (before the contra-minus-ipsi subtraction) are shown in supplemental Figure S2.

The N2pc began approximately 145 ms after stimulus onset for all eccentricities. N2pc amplitude was comparable across all eccentricities except the most extreme one (8°), which produced a markedly smaller N2pc. The N2pc was followed by a contralateral positivity, leading the voltage to cross the zero line between approximately 240 and 320 ms, depending on the eccentricity. The time of the negative-to-positive transition decreased monotonically, and the amplitude of the positivity increased monotonically, between the 0° eccentricity and the 8° eccentricity. This post-N2pc positivity (PNP) is at least superficially similar to contralateral positivities reported in similar experiments (e.g., Hilimire & Corballis, 2014; Jannati, Gaspar, & McDonald, 2013; Sawaki, Geng, & Luck, 2012).

3.2.1 N2pc Statistical Analyses—

Mean amplitudes from the N2pc time window are shown in Figure 6A. A one-way ANOVA yielded a significant main effect of eccentricity ($F(5, 95) = 3.12$, $p_{HF} = .004$). FDR-corrected paired comparisons between successive

eccentricities (comparing 0° to 0.05°, 0.05° to 1°, etc.) indicated that the eccentricity effect was mainly a result of a drop in amplitude at 8° (see Table 1). Specifically, there were no significant differences between neighboring eccentricities except between 4° and 8°, $t(19) = -2.93$, $p = .008$.

One-sample t-tests comparing the voltage to zero for each eccentricity indicated the presence of a significant negativity for all eccentricities except 8°, for which N2pc amplitude was not significantly different from zero (see Table 2).

3.2.2 PNP Statistical Analyses—Mean amplitudes from the PNP time window are shown in Figure 6B. Although PNP amplitude appeared to increase progressively as the eccentricity increased, a one-way repeated measures ANOVA did not yield a significant main effect of eccentricity ($F(5, 95) = 1.63$, $p_{HF} = .178$). Moreover, FDR-corrected paired comparisons between successive eccentricities revealed no significant differences between adjacent eccentricities (see Table 1 for details).

However, a post hoc comparison of the 0° and 8° eccentricities did yield a significant difference ($t(19) = -2.57$, $p = .019$, $d_{av} = -0.64$ (95% CI: −1.10 - −0.11). Moreover, a one-sample t-test on the mean PNP amplitude in each condition revealed a significant positivity for the 2°, 4°, and 8° conditions, but not for the 0°, 0.05°, and 1° conditions (see Table 2). Thus, evidence for an effect of eccentricity on PNP amplitude was mixed.

Eccentricity-dependent eye movements were present during the PNP analysis window (see Figure 3), raising the possibility that PNP effects were influenced by eye movements. However, as discussed in Section 4, the timing, direction, and size of the eye movements suggest that any effect is likely to be relatively minor.

3.3 Exploratory Analyses

Our a priori analyses focused on the amplitudes of the N2pc and PNP components, but the observed waveforms suggested that latencies were also impacted by eccentricity. We therefore conducted post hoc exploratory analyses of the N2pc and PNP latencies. The procedures and parameters used for these analyses were determined a posteriori, so the results of these analyses should be treated as merely suggestive rather than definitive. Further experiments that specifically test for these effects would be needed before any strong conclusions could be drawn.

Because onset latencies are difficult to measure robustly in single-participant data, the jackknife statistical approach was used (Miller, Patterson, & Ulrich, 1998; Ulrich & Miller, 2001).

3.3.1 N2pc Latency—To quantify the effect of eccentricity on N2pc onset latency, we measured the 50% peak latency of the N2pc (i.e., the time at which the amplitude reached 50% of the peak amplitude; see Luck, 2014). Because N2pc amplitude was very small for the 8° eccentricity, making the latency difficult to measure, these trials were excluded from the N2pc onset latency analyses.

The mean N2pc onset latency values are shown in Figure 5A. N2pc onset latency decreased slightly with increasing eccentricity, but this effect was not significant in a one-way ANOVA ($F_{corrected}(5,95) = 0.43$, $p_{hf} = .648$). FDR-corrected paired comparisons between adjacent eccentricities revealed no significant differences (see Table 1) except between 1° and 2° ($t_{corrected}(19) = 1.85$, $p = .039$). However, there was a significant decrease in latency between 0° and 4° ($t_{corrected}(19) = 3.25$, $p = .002$). Thus, N2pc latency appeared to decrease slightly at larger eccentricities, but the statistical evidence for this was mixed.

3.3.2 Polarity Transition Latency—Because of the overlapping N2pc component, it was not possible to obtain a pure estimate of PNP onset latency. Consequently, we instead focused on the time of the transition between N2pc and PNP, which we quantified as the *polarity transition latency* (the time at which the ERP transitioned from a negative voltage to a positive voltage between the N2pc and PNP). We again used the jackknife technique to obtain more robust measurements.

Like N2pc onset latency, the polarity transition latency generally decreased as the eccentricity increased (see Figure 7B). A one way ANOVA yielded a significant main effect of eccentricity ($F_{corrected}(5,95) = 0.367$, $p_{hf} = .038$). FDR-corrected paired comparisons between successive eccentricities revealed no significant differences in latency in any successive pair (see Table 1), except between 0.05° and 1° ($t_{corrected}(19) = 2.37$, $p = .035$). However, there was a significant decrease in latency between the 0° and 8° conditions ($t_{corrected}(19) = 3.72$, $p < .001$). Thus, the polarity transition latency appeared to decrease slightly at larger eccentricities, but the statistical evidence for this was somewhat mixed.

3.3.4 Lateralized Alpha Suppression—Analyses of alpha-band activity are provided in the online supplementary materials. Briefly, we found a small but statistically significant suppression of alpha-band activity at contralateral relative to ipsilateral electrode sites approximately 500 ms after target onset (see Figure S3.2). No significant effects of eccentricity or magnification were obtained, but the overall alpha lateralization may have been too small to detect modulations by these factors.

4. Discussion

This study was designed to assess the effects of eccentricity on N2pc amplitude. We found that the N2pc was robustly present for stimuli immediately adjacent to the midline, with no significant change in amplitude up to 4°. That is, a robust N2pc was observed for stimuli that were so close to the midline that they presumably fell into receptive fields in both hemispheres. However, N2pc amplitude declined precipitously for stimuli at 8°. The positivity following N2pc (PNP) showed some evidence of increased amplitude at greater eccentricities. Both the onset of the N2pc component and the transition between the N2pc and PNP tended to become earlier at greater eccentricities, but the statistical evidence for these effects was mixed.

Although we did not find a significant difference in amplitude across the 0°−4° conditions, we are not claiming that N2pc amplitude is exactly identical over this range of eccentricities, which would require proving the null hypothesis. Our main claim regarding this range of

eccentricities is that a robust N2pc is elicited by stimuli throughout this range, including stimuli presented very near the vertical meridian. This result suggests that hemispheric differences in processing occur even for stimuli that presumably fall within the receptive fields of neurons in both hemispheres.

Our finding of a substantial drop in N2pc amplitude at 8° is somewhat inconsistent with the findings of Schaffer et al. (2011), who did not find a large decline in the N2pc elicited by texture discontinuities at an eccentricity of 7°. However, there are multiple differences between our experiment and those conducted by Schaffer et al. that could explain the different results. First, we used stimuli that are more typical for N2pc experiments and that controlled for low-level differences in visual energy across the visual hemifields. Furthermore, task difficulty remained relatively consistent across eccentricities in the present study, and thus our findings may reflect a purer measure of the effect of eccentricity.

From a practical standpoint, these results indicate that future N2pc experiments can safely use stimuli at small-to-moderate eccentricities without impacting the ability to detect the component. Specifically, the current results support the use of stimuli that range from being directly adjacent to the midline to those having an eccentricity of up to 4°. This may be particularly useful for studies using stimuli that are difficult to perceive outside the parafoveal region, such as faces. However, stimuli with an eccentricity of 8° or more would be expected to produce a very small N2pc, leading to poor sensitivity and low statistical power. Unfortunately, the present design does not provide any information about eccentricities that fall between 4° and 8°.

The observed pattern of N2pc amplitudes is also consistent with the neuroanatomical characteristics of the likely sources of the N2pc. The concentration of RFs in the center of gaze in these regions could explain the significantly smaller N2pc amplitude for the 8° eccentricity. That is, few RFs in higher-level ventral visual areas extend that far into the periphery (Dumoulin & Wandell, 2008; Gross et al., 1972), so stimuli more than 8° from the midline are represented by a small number of neurons in these areas. This might lead to a reduced overall neural response from these areas, resulting in a smaller N2pc. Stimuli presented at more moderate eccentricities (i.e., ≤4°) fall within the more numerous parafoveal RFs, resulting in a more robust N2pc.

The large N2pc amplitude for stimuli adjacent to the midline might seem puzzling given that many neurons in higher-level regions of visual cortex have RFs that extend over the midline and into the ipsilateral visual field. However, this result may be explained by the findings of Chelazzi et al. (1998), who reported that neurons with bilateral RFs are biased to represent the contralateral items in a bilateral display. Because our stimulus arrays were always symmetrical (i.e., stimuli were presented at the same eccentricity on both sides of the display), trials with near stimuli would result in the attended item being represented primarily by the contralateral hemisphere, which would lead to the lateralized activation needed for the N2pc.

The use of symmetrical displays was important for avoiding any lateralized differences in stimulus energy that might lead to spurious contralateral-minus-ipsilateral differences.

However, this design confounds differences in target eccentricity with differences in distractor eccentricity. In other words, as the target eccentricity increased, so did the distractor eccentricity and the distance between the target and distractor, making it is difficult to know which of these factors was responsible for the observed eccentricity effects. However, the target was also flanked by distractors immediately above and below it, which presumably had a much larger effect on target processing than the distractors in the opposite visual field. Consequently, it seems unlikely that the eccentricity of the opposite-field distractors or the distance between the target and the opposite-field distractors would have had much influence on the results. It is more parsimonious to assume that the effects were driven by the eccentricity of the target and the same-hemifield distractors. However, additional research would be needed to draw this conclusion with certainty.

Another interesting finding was that the effects of eccentricity were quite different for the PNP and N2pc. Whereas the N2pc was largely identical between the 0° and 4° eccentricities and then dropped off at 8°, the PNP showed some signs of an increase in amplitude as eccentricity increased. It is possible that this difference between the N2pc and PNP reflects a functional and/or anatomical difference in the sources of the two components, which may indicate that the PNP is a result of a different process than the N2pc. In theory, this issue could be explored by asking whether the N2pc and PNP have different scalp distributions. Unfortunately, it is technically difficult to compare scalp distributions (Urbach & Kutas, 2002, 2006). Moreover, the electrode density used in the present study was probably insufficient to detect any differences in scalp distribution between the N2pc and PNP given that the distributions were generally quite similar.

It should be noted that the overlap between the N2pc and PNP makes it difficult to attribute the observed PNP eccentricity effects to the PNP itself. That is, effects of eccentricity on the duration of the N2pc component could produce apparent changes in the onset time and amplitude of the PNP.

Furthermore, although we were able to remove trials with eye movements during the N2pc time window, it was not possible to do the same during PNP time window without rejecting too many trials. Thus, it possible that the PNP effects were partially a result of eye movements. However, there are several reasons to believe that any effects of eye movements on the PNP would have been quite small.

The effects of eye movements can be broken down into two parts. First, the corneal-retinal potential within each eye produces a voltage deflection at the scalp when the eyes rotate, which simply sums with brain-related potentials. These artifactual potentials should be largely removed by ICA correction (Drisdelle et al., 2017; Mennes et al., 2010). and any remaining activity would be characterized by a contralateral negativity and thus cannot be the primary source of the increased positivity reported during the PNP time window. Second, any eye movements that occur while the stimulus is present would result in a change in visual input, because the stimuli would now fall on different parts of the retina. It is possible that this change in visual information affected the PNP effects. However, the eye movements were small relative to the eccentricity of the stimuli. For example, the average eye rotation during the PNP period was less than 0.5° when the targets were presented at 8° (see Figure

3). Moreover, the timing of the changes in eye position were very different from the timing of the PNP effect. Thus, although we cannot rule out the possibility that eye movements had some effect on the pattern of PNP results, this effect was almost certainly quite small.

Exploratory analyses indicated that the N2pc latency and polarity transition latency became progressively shorter as eccentricity increased (but these effects should be treated with caution given that they were exploratory). Ordinarily, one would expect longer latencies at greater eccentricities given that reaction times often increase with eccentricity (Carrasco, Evert, Chang, & Katz, 1995; Carrasco, Mclean, Katz, & Friedert, 1998). One possible explanation for the longer latencies at smaller eccentricities is that the opposite-hemifield distractors may have had more impact on the allocation of attention for stimuli very close to the midline. However, more research would be needed before making strong claims about these latency effects.

Supplementary Material

Refer to Web version on PubMed Central for supplementary material.

Acknowledgments

This study was made possible by grant R01MH076226 from the National Institute of Mental Health.

References

Bacigalupo F, & Luck SJ (2019). Lateralized Suppression of Alpha-Band EEG Activity As a Mechanism of Target Processing. The Journal of Neuroscience, 39(5), 900–917. 10.1523/JNEUROSCI.0183-18.2018 [PubMed: 30523067]

Benjamini Y, Krieger AM, & Yekutieli D (2006). Adaptive linear step-up procedures that control the false discovery rate. Biometrika, 93(3), 491–507. 10.1093/biomet/93.3.491

Brainard DH (1997). The Psychophysics Toolbox. Spatial Vision, 10(4), 433–436. 10.1163/156856897X00357 [PubMed: 9176952]

Carrasco M, Evert DL, Chang I, & Katz SM (1995). The eccentricity effect : Target eccentricity affects performance on conjunction searches, 57(8), 1241–1261.

Carrasco M, Mcelree B, Denisova K, & Giordano AM (2003). Speed of visual processing increases with eccentricity. Nature Neuroscience, 87, 1–2. 10.1038/nn1079

Carrasco M, Mclean TL, Katz SM, & Friedert KS (1998). Feature Asymmetries in Visual Search : Effects of Display Duration, Target Eccentricity, Orientation and Spatial Frequency *, 38(3), 347–374.

Chelazzi L, Duncan J, Miller EK, & Desimone R (1998). Responses of Neurons in Inferior Temporal Cortex During Memory- Guided Visual Search. 10.1152/jn.1998.80.6.2918

Drisdelle BL, Aubin S, & Jolicoeur P (2017). Dealing with ocular artifacts on lateralized ERPs in studies of visual-spatial attention and memory: ICA correction versus epoch rejection. Psychophysiology, 54(1), 83–99. 10.1111/psyp.12675 [PubMed: 28000252]

Dumoulin SO, & Wandell BA (2008). Population receptive field estimates in human visual cortex. NeuroImage, 39(2), 647–660. 10.1016/j.neuroimage.2007.09.034 [PubMed: 17977024]

Groppe DM, Urbach TP, & Kutas M (2011a). Mass univariate analysis of event-related brain potentials/fields I: A critical tutorial review. Psychophysiology, 48(12), 1711–1725. 10.1111/j.1469-8986.2011.01273.x [PubMed: 21895683]

Groppe DM, Urbach TP, & Kutas M (2011b). Mass univariate analysis of event-related brain potentials/fields II: Simulation studies. Psychophysiology, 48(12), 1726–1737. 10.1111/j.1469-8986.2011.01272.x [PubMed: 21895684]

Gross CG, Roch-Miranda CE, & Bender DB (1972). Visual Cortex Properties of Neurons in Inferotemporal of the Macaque. Journal of Neurophysiology, 35(1), 96–111. [PubMed: 4621506]

Hickey C, Di Lollo V, & Mcdonald JJ (2008). Electrophysiological Indices of Target and Distractor Processing in Visual Search, 760–775.

Hilimire MR, & Corballis PM (2014). Event-related potentials reveal the effect of prior knowledge on competition for representation and attentional capture. Psychophysiology, 51(1), 22–35. 10.1111/psyp.12154 [PubMed: 24147640]

Hopf J, Luck SJ, Boelmans K, Schoenfeld MA, Boehler CN, Rieger J, & Heinze H (2006). The Neural Site of Attention Matches the Spatial Scale of Perception, 26(13), 3532–3540. 10.1523/JNEUROSCI.4510-05.2006

Hopf J, Luck SJ, Girelli M, Hangner T, Mangun GR, Scheich H, & Heinze H-J (2000). Neural Sources of Focused Attention in Visual Search. Cerebral Cortex, 10(12), 1233–1241. 10.1093/cercor/10.12.1233 [PubMed: 11073872]

Jannati A, Gaspar JM, & McDonald JJ (2013). Tracking target and distractor processing in fixed-feature visual search: Evidence from human electrophysiology. Journal of Experimental Psychology: Human Perception and Performance, 39(6), 1713–1730. 10.1037/a0032251 [PubMed: 23527999]

Lawrence MA (2013). Easy analysis and visualization of factorial experiments. Retrieved from https://cran.r-project.org/package=ez

Lins OG, Picton TW, Berg P, & Scherg M (1993). Ocular artifacts in EEG and event-related potentials I: Scalp topography. Brain Topography, 6(1), 51–63. 10.1007/BF01234127 [PubMed: 8260327]

Logan GD (1998). Toward an instance thepry of automatization. Psychological Review, 95(4), 492–527.

Luck SJ (2014). An Introduction to the Event-Related Potential Technique, second edition The MIT Press 10.1118/1.4736938

Luck SJ, & Gaspelin N (2017). How to get statistically significant effects in any ERP experiment (and why you shouldn't). Psychophysiology, 54(1), 146–157. 10.1111/psyp.12639 [PubMed: 28000253]

Luck SJ, Girelli M, McDermott MT, & Ford MA (1997). Bridging the gap between monkey neurophysiology and human perception: an ambiguity resolution theory of visual selective attention. Cognit Psychol, 33(1), 64–87. 10.1006/cogp.1997.0660 [PubMed: 9212722]

Mennes M, Wouters H, Vanrumste B, Lagae L, & Stiers P (2010). Validation of ICA as a tool to remove eye movement artifacts from EEG/ERP. Psychophysiology, 47(6), 1142–1150. 10.1111/j.1469-8986.2010.01015.x [PubMed: 20409015]

Miller J, Patterson TUI, & Ulrich R (1998). Jackknife-based method for measuring LRP onset latency differences, 99–115.

Pelli DG (1997). The VideoToolbox software for visual psychophysics: Transforming numbers into movies. Spatial Vision, 10(4), 437–442. 10.1163/156856897X00366 [PubMed: 9176953]

R Core Team. (2016). R: A language and environment for statistical computing.

Sawaki R, Geng JJ, & Luck SJ (2012). A Common Neural Mechanism for Preventing and Terminating the Allocation of Attention. Journal of Neuroscience, 32(31), 10725–10736. 10.1523/JNEUROSCI.1864-12.2012 [PubMed: 22855820]

Schaffer S, Schubö A, & Meinecke C (2011). Electrophysiological correlates of target eccentricity in texture segmentation. International Journal of Psychophysiology, 80, 198–209. [PubMed: 21419177]

Ulrich R, & Miller J (2001). Using the jackknife-based scoring method for measuring LRP onset effects in factorial designs, 816–827.

Urbach TP, & Kutas M (2002). The intractability of scaling scalp distributions to infer neuroelectric sources, c, 791–808.

Urbach TP, & Kutas M (2006). Interpreting event-related brain potential (ERP) distributions : Implications of baseline potentials and variability with application to amplitude normalization by vector scaling, 72, 333–343. 10.1016/j.biopsycho.2005.11.012

Woodman GF, & Luck SJ (2003). Serial deployment of attention during visual search. Journal of Experimental Psychology: Human Perception and Performance, 29(1), 121–138. 10.1037/0096-1523.29.1.121 [PubMed: 12669752]

Worden MS, Foxe JJ, Wang N, & Simpson GV (2000). Anticipatory Biasing of Visuospatial Attention Indexed by Retinotopically Specific α-Band Electroencephalography Increases over Occipital Cortex, 20, 1–6.

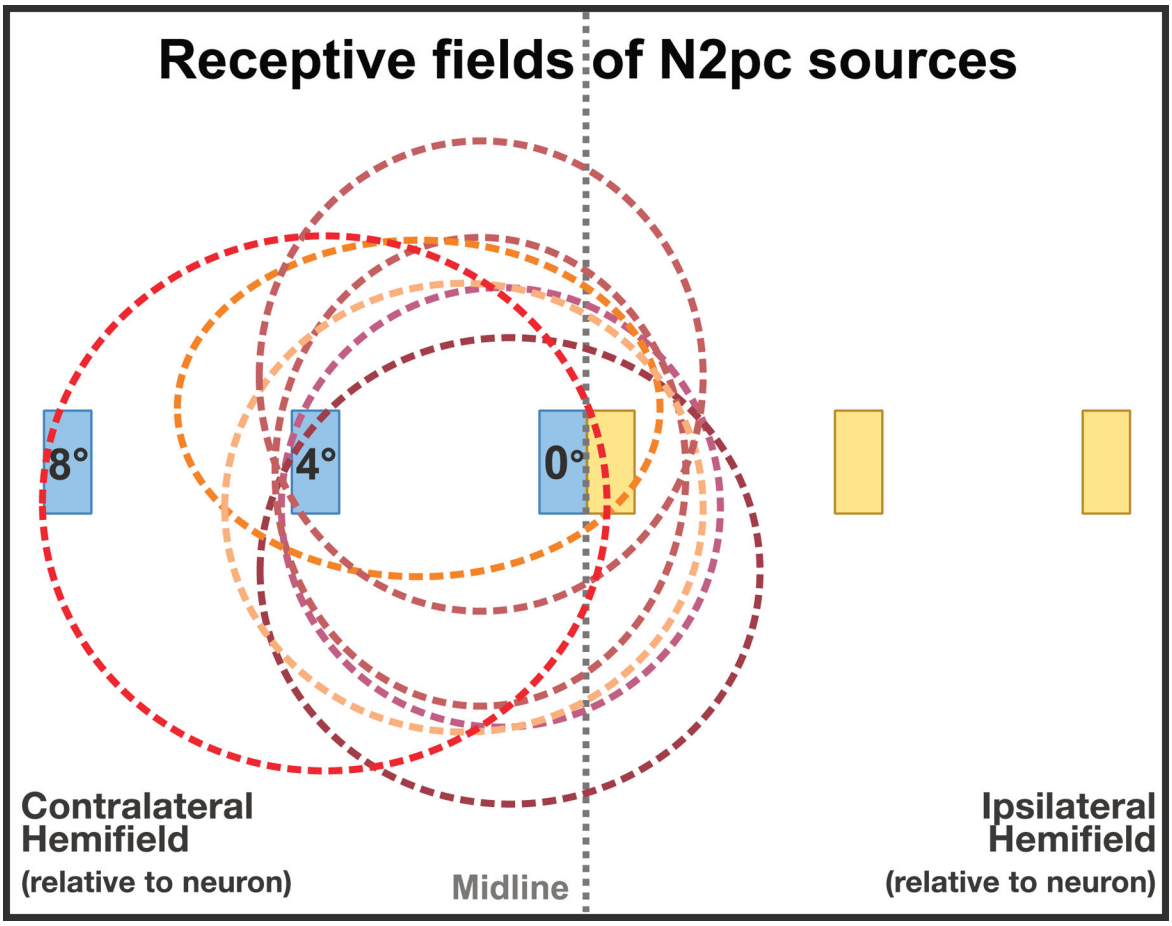

Figure 1:
Schematic representation of typical receptive fields in the middle- to high-level areas of the ventral processing stream that are thought to be the sources of the N2pc. Note that the stimuli at 8° fall inside relatively few receptive fields, which might be expected to decrease N2pc amplitude. In addition, stimuli near the midline will fall inside receptive fields in both the contralateral and ipsilateral hemispheres, which might also be expected to decrease N2pc amplitude (measured as the contralateral-minus-ipsilateral difference).

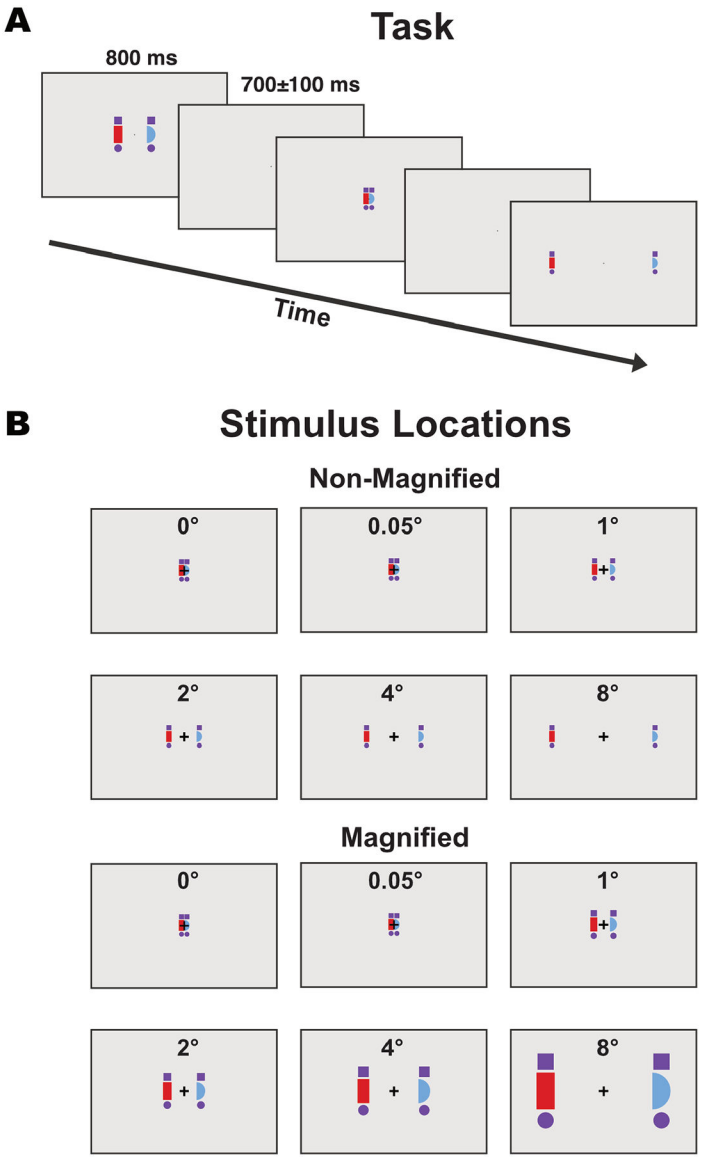

Figure 2:

Example stimulus sequence (A) and all possible stimulus positions and sizes (B). Participants were instructed to pay attention to the red or blue shape (counterbalanced across blocks) and to indicate with a button press whether the attended shape was a hemicircle or a rectangle. Stimuli are drawn to scale (except for the fixation point, which was smaller than shown here). The outline around each image corresponds to the edges of the video monitor.

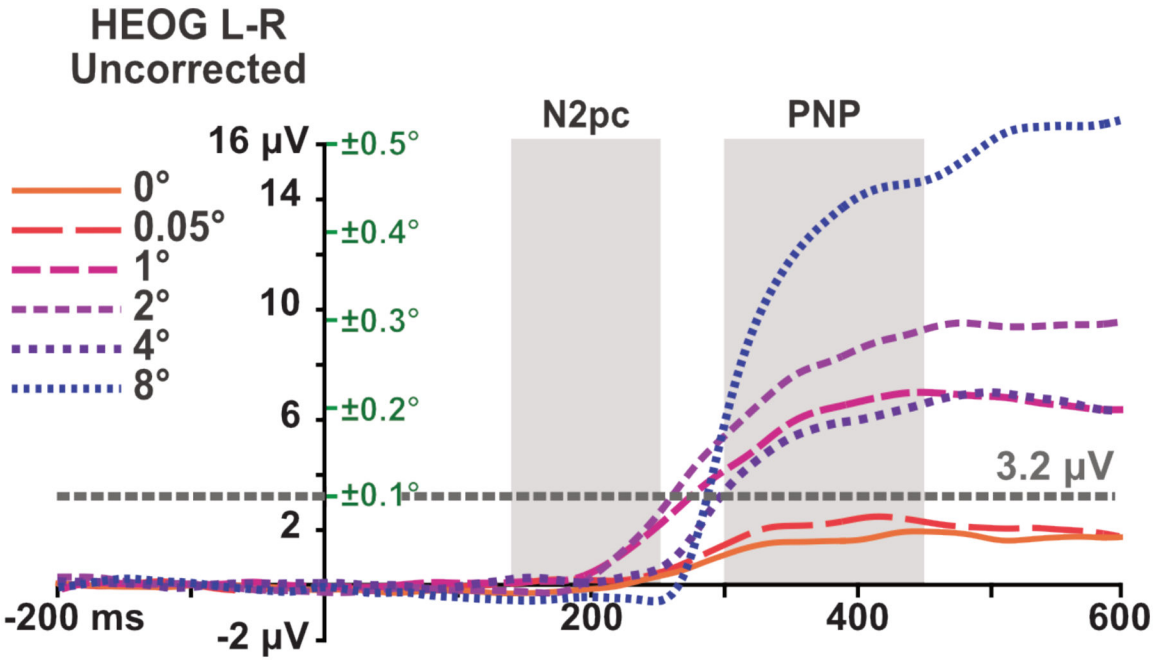

Figure 3:

Residual HEOG activity (left-target minus right-target difference wave) after artifact rejection but without ICA correction. The grey areas represent the time windows that were used for analyzing the N2pc and PNP respectively. The grey line at 3.2 µV corresponds to an average eye rotation of ±0.1° (on the basis of the normative values provided by Lins et al., 1993). The green values on the right of the y-axis indicate the eye movement size that would correspond to a particular HEOG amplitude.

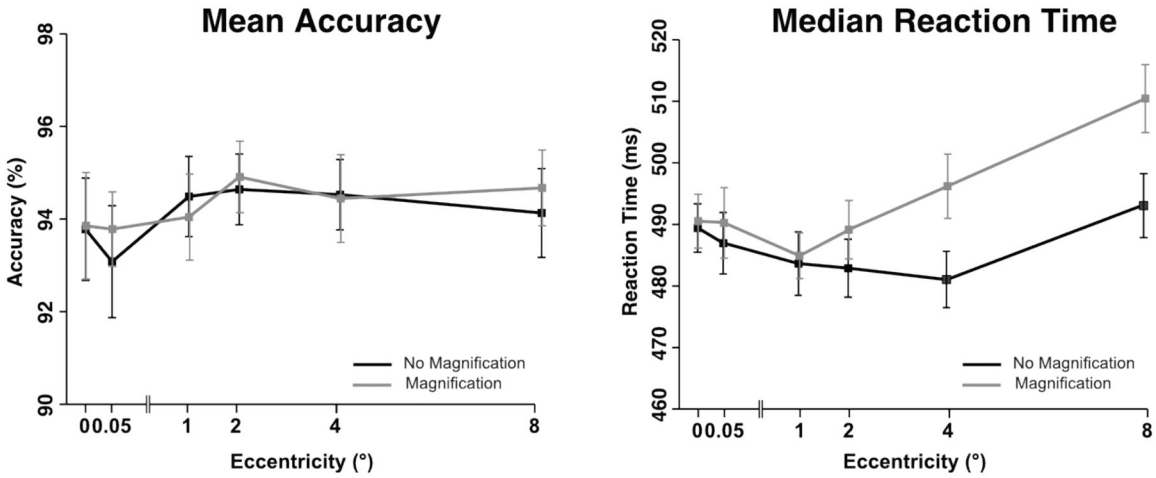

Figure 4:

Accuracy (A) and reaction time (B) as a function of eccentricity and magnification. Error bars represent the within-subjects 95% confidence interval (Morey, 2008).

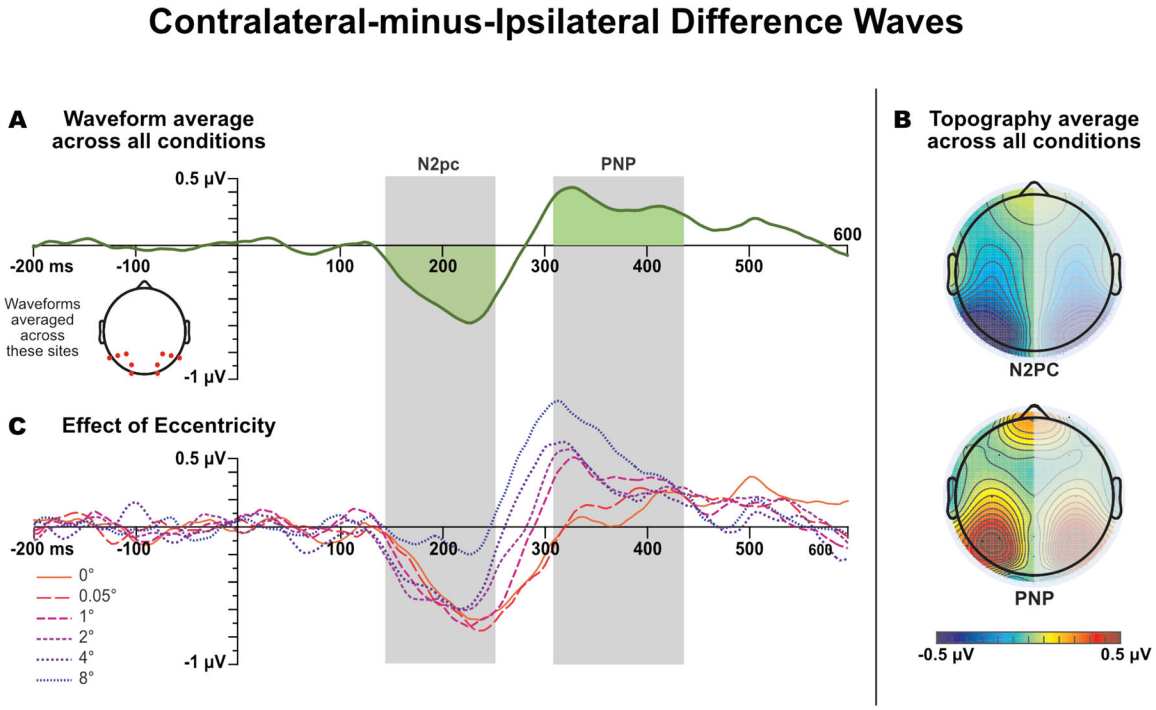

Figure 5:

Grand average contralateral-minus-ipsilateral difference waves, averaged across the posterior electrodes. (A) Waveforms collapsed across all factors to determine the overall time windows for measuring N2pc and PNP mean amplitude. The grey bands show the time windows in which activity averaged across eccentricities was significantly different from zero (which were then used for the single-eccentricity measurements). (B) Topography of the mean amplitude in these time windows, mirrored across the left and right hemispheres (because the difference waves were collapsed across hemispheres). (C) Waveforms separated as a function of eccentricity, but collapsed across magnification. All waveforms shown here were low-pass filtered for visual clarity (noncausal Butterworth low-pass filter, half-amplitude cutoff = 20 Hz, slope = 24 dB/octave).

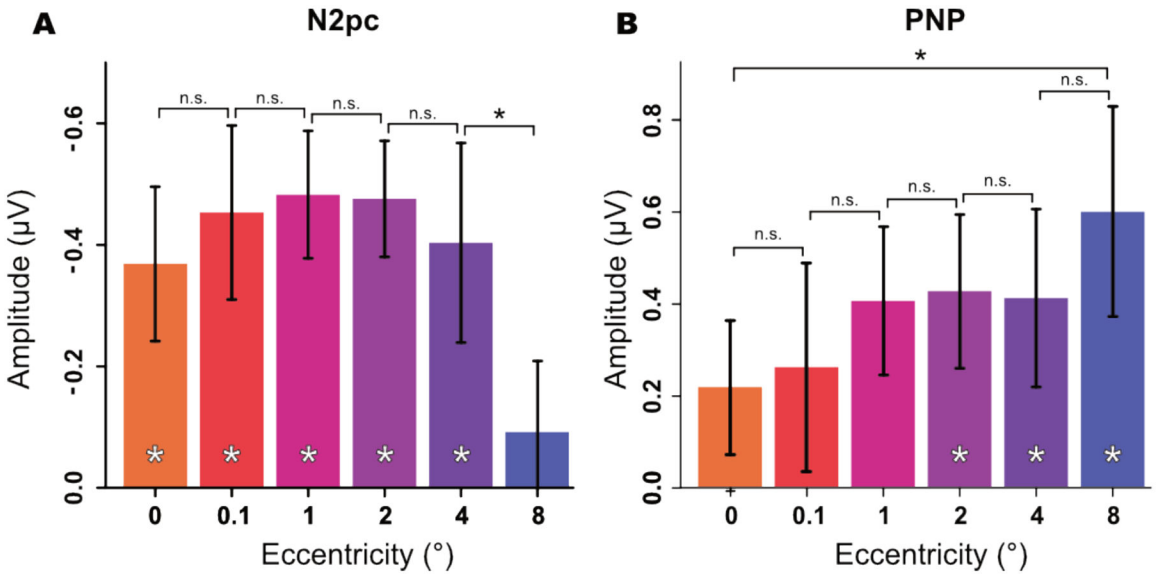

Figure 6:

Mean amplitude as a function of eccentricity during the N2pc (A) and PNP (B) time windows. Error bars represent the within-subjects 95% confidence interval. A significant difference ($p < .05$) between two means is indicated by a black asterisk, and a significant difference of a single mean from zero is indicated by a white asterisk (after FDR correction).

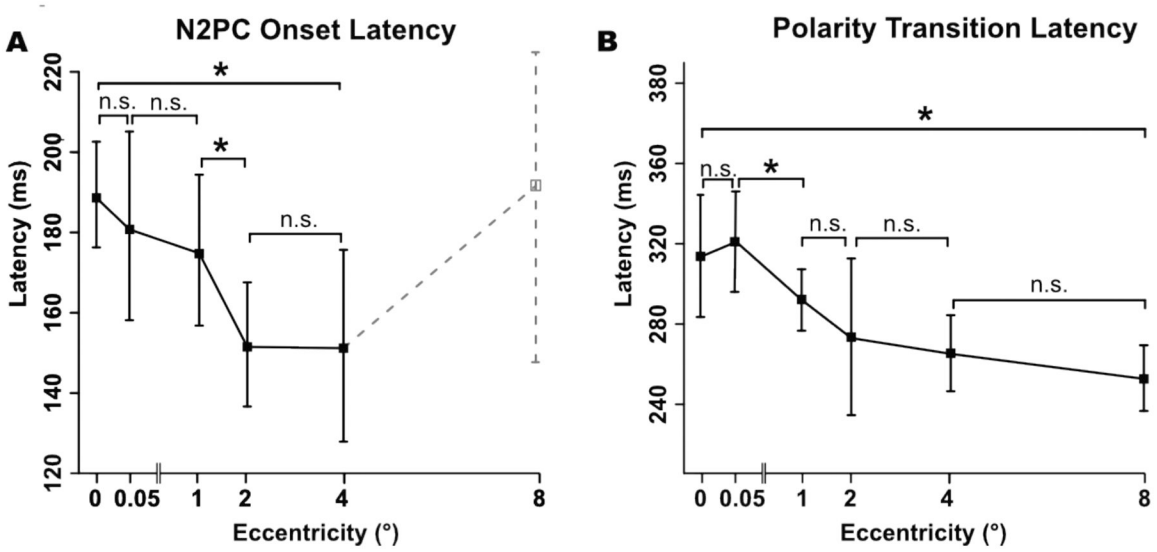

Figure 7:

N2pc onset latency (A) and polarity transition latency (B) as a function of eccentricity. Error bars represent the within-subjects 95% confidence interval. Asterisks denote a significant difference ($p < .05$) between adjacent eccentricities after FDR correction. Note that the N2pc onset latency at 8° is not meaningful given that the amplitude was near zero for that eccentricity, so broken lines are used for N2pc onset latency that eccentricity.

Table 1:

t scores and p-values for the pairwise comparisons. An asterisk denotes that the comparison was significant ($p < .05$) after FDR correction. Effect sizes are given as the 95% confidence interval of the Cohen's d for correlated samples (d_{av}) as defined in Lakens (2013). For latency measures, we report the values after correcting for the jackknife procedure. Since there is no agreed-upon jackknife correction for d_{av}, effect sizes are not reported for latency measures.

			Measurement				
			N2pc	**PNP**	**N2pc latency**	**Polarity Transition Latency**	**Lateralized Alpha Suppression**
Eccentricities Being Compared	**0° vs 0.05°**	**t(19)**	1.50	−0.29	0.81	0.45	−1.13
		p	0.149	0.778	0.21	0.34	0.273
		d_{av} (95% CI)	0.30 (−0.12 – 0.73)	−0.05 (−0.38 – 0.29)	–	–	−0.29 (−0.83 – 0.25)
	0.05° vs 1°	**t(19)**	0.02	−1.31	0.52	2.37	1.34
		p	0.983	0.203	0.304	0.035*	0.196
		d_{av} (95% CI)	0.01 (−0.52 – 0.54)	−0.28 (−0.71 – 0.16)	–	–	0.50 (−0.28 – 1.28)
	1° vs 2°	**t(19)**	−0.49	0.09	1.85	0.91	0.70
		p	0.631	0.931	0.040*	0.203	0.478
		d_{av} (95% CI)	−0.027 (−0.39 – 0.24)	−0.01 (−0.31 – 0.29)	–	–	0.16 (–0.30 – 0.60)
	2° vs 4°	**t(19)**	--0.53	0.60	0.04	0.43	−1.26
		p	0.604	0.558	0.486	0.343	0.223
		d_{av} (95% CI)	−0.11 (−0.55 – 0.33)	0.10 (−0.26 – 0.46)	–	–	0.23 (−0.62 – 0.15)
	4° vs 8°	**t(19)**	−2.94	−1.23	–	1.29	−1.79
		p	0.008*	0.234	–	0.129	0.089
		d_{av} (95% CI)	−0.62 −1.07 – −0.18	−0.28 (−0.75 – 0.20)	–	–	−0.42 (−0.91 – 0.07)

Table 2:

t-scores and p-values for one-sample t-tests assessing whether the amplitude was different from zero. The asterisk denotes significance after FDR correction

			N2pc	PNP
Eccentricity	**0°**	**Mean**	−0.370	0.227
		SD	0.297	0.389
		SME	0.051	0.054
		t(19)	−5.57	2.61
		p	<0.001*	0.017
	0.05°	**Mean**	−0.457	0.248
		SD	0.274	0.528
		SME	0.051	0.054
		t(19)	−7.47	2.10
		p	<0.001*	0.049
	1°	**Mean**	−0.483	0.418
		SD	0.427	0.686
		SME	0.052	0.0543
		t(19)	−4.81	2.72
		p	<0.001*	0.013
	2°	**Mean**	−0.459	0.426
		SD	0.365	0.609
		SME	0.052	0.055
		t(19)	−5.25	3.13
		p	<0.001*	0.006*
	4°	**Mean**	−0.429	0.365
		SD	0.445	0.591
		SME	0.051	0.053
		t(19)	−3.86	2.76
		p	<0.001*	0.013*
	8°	**Mean**	−0.127	0.527
		SD	0.375	0.581
		SME	0.050	0.054
		t(19)	−1.52	4.06
		p	0.146	<0.001*